THE JOURNAL OF BIOLOGICAL CHEMISTRY VOL. 283, NO. 26, pp. 18040–18047, June 27, 2008

Differential Sorting and Golgi Export Requirements for Raft-associated and Raft-independent Apical Proteins along the Biosynthetic Pathway*

Received for publication, March 14, 2008, and in revised form, April 16, 2008 Published, JBC Papers in Press, April 22, 2008, DOI 10.1074/jbc.M802048200

Christopher J. Guerriero[‡1,2], **Yumei Lai**[‡1], **and Ora A. Weisz**[‡§3]

From the Departments of [‡]*Medicine and* [§]*Cell Biology and Physiology, University of Pittsburgh School of Medicine, Pittsburgh, Pennsylvania 15261*

Sorting signals for apically destined proteins are highly diverse and can be present within the luminal, membrane-associated, and cytoplasmic domains of these proteins. A subset of apical proteins partition into detergent-resistant membranes, and the association of these proteins with glycolipid-enriched microdomains or lipid rafts may be important for their proper targeting. Recently, we observed that raft-associated and raft-independent apical proteins take different routes to the apical surface of polarized Madin-Darby canine kidney cells (Cresawn, K. O., Potter, B. A., Oztan, A., Guerriero, C. J., Ihrke, G., Goldenring, J. R., Apodaca, G., and Weisz, O. A. (2007) *EMBO J.* 26, 3737–3748). Here we reconstituted *in vitro* the export of raft-associated and raft-independent markers staged intracellularly at 19 °C. Surprisingly, whereas release of the raft-associated protein influenza hemagglutinin was dependent on the addition of an ATP-regenerating system and cytosol, release of a yellow fluorescent protein (YFP)-tagged raft-independent protein (the 75-kDa neurotrophin receptor; YFP-p75) was efficient even in the absence of these constituents. Subsequent studies suggested that YFP-p75 is released from the *trans*-Golgi network in fragile tubules that do not withstand isolation procedures. Moreover, immunofluorescence analysis revealed that hemagglutinin and YFP-p75 segregate into distinct subdomains of the Golgi complex at 19 °C. Our data suggest that raft-associated and raft-independent proteins accumulate at distinct intracellular sites upon low temperature staging, and that upon warming, they exit these compartments in transport carriers that have very different membrane characteristics and morphologies.

Efficient sorting of newly synthesized proteins along the biosynthetic pathway is critical for cell function. An additional requirement for maintaining the function and integrity of polarized epithelial cells is the selective targeting of newly synthesized cargo to differentiated apical and basolateral cell surface domains. This is accomplished by the recognition of sorting information within individual proteins that confers their segregation into distinct post-Golgi transport containers (1, 2). Basolateral sorting signals generally consist of short peptide sequences in the cytoplasmic domains of these proteins that sometimes fit the consensus for binding to adaptor protein complex subunits. In contrast, apical sorting signals are more diverse. These signals can localize to the luminal, transmembrane, or cytoplasmic domains of apical proteins. Post-translational modifications, including *N*- and *O*-linked glycans (*e.g.* on endolyn and the 75-kDa neurotrophin receptor (p75), respectively (3)), and glycosylphosphatidylinositol anchors have been described as apical sorting signals. For some proteins, including influenza hemagglutinin (HA),[4] apical sorting is conferred by sorting information within the transmembrane domain (4). HA- and glycosylphosphatidylinositol-anchored proteins are partially insoluble in cold Triton X-100 and preferentially associate with glycolipid-enriched microdomains (also known as lipid rafts or detergent-resistant membranes), although how this association plays a role in apical targeting is not yet understood (5).

The diversity in apical sorting signals suggests that proteins with distinct classes of sorting signals might be sorted and packaged into distinct transport carriers leaving the *trans*-Golgi network (TGN). In fact, there is growing evidence, including data from our own lab, to suggest the existence of multiple pathways from the TGN to the apical surface. These pathways have been best described in models comparing the trafficking raft-associated *versus* raft-independent apical markers. Jacob and Naim (6) investigated the trafficking mechanisms of sucrose-isomaltase, which associates with lipid rafts and the raft-independent marker lactase-phlorizin hydrolase. These two proteins initially exited the TGN together in a large transport vesicle, which then budded into smaller vesicles preferentially containing either protein. Subsequent studies demonstrated a selective role for myosin 1A-based motility in the surface delivery of sucrase-isomaltase (7). Similarly, our lab found that post-Golgi delivery of the raft-associated HA was regulated by an N-WASP-dependent pathway, whereas delivery of p75, a raft-independent protein, was unaffected (8).

* This work was supported, in whole or in part, by National Institutes of Health Grant DK054407 (to O. A. W.). The costs of publication of this article were defrayed in part by the payment of page charges. This article must therefore be hereby marked "*advertisement*" in accordance with 18 U.S.C. Section 1734 solely to indicate this fact.

[1] These authors contributed equally to this work.

[2] Supported by an American Heart Association predoctoral fellowship.

[3] To whom correspondence should be addressed: Renal-Electrolyte Division, University of Pittsburgh School of Medicine, 3550 Terrace St., Pittsburgh PA 15261. E-mail: weisz@pitt.edu.

[4] The abbreviations used are: HA, influenza hemagglutinin; GFP, green fluorescent protein; MDCK, Madin-Darby canine kidney; TGN, *trans*-Golgi network; VSV-G, vesicular stomatitis virus glycoprotein; YFP, yellow fluorescent protein.

In addition to the apparent sorting of raft-associated and raft-independent proteins into distinct transport carriers, we have recently found that these two populations of proteins take different routes to the apical membrane (9). Interestingly, the biosynthetic route of each of these classes of proteins appears to intersect with a different population of endosomes in polarized MDCK cells. Whereas raft-associated proteins including HA- and glycosylphosphatidylinositol-anchored proteins appear to transit early endocytic compartments that are accessible to apically internalized wheat germ agglutinin, delivery of apical membrane proteins with *N*-glycan-dependent sorting information proceeds through the rab11-positive, transferrin-negative apical recycling endosome (9). In contrast, the glycoprotein of vesicular stomatitis virus (VSV-G) has been shown to transit transferrin positive recycling endosomes in MDCK cells prior to surface delivery (9, 10), whereas newly synthesized low density lipoprotein receptor appears to bypass this compartment (11).

We have begun to dissect the mechanisms that mediate segregation of newly synthesized proteins along the biosynthetic pathway. To this end, we have developed *in vitro* assays to reconstitute the export of newly synthesized raft-associated and non-raft-associated apical markers into post-Golgi transport containers. Our results suggest that carriers enriched in these distinct cargoes have very different morphologies and that their formation occurs from distinct subdomains of the Golgi via different mechanisms.

MATERIALS AND METHODS

Cell Lines, Adenoviral Infection, and Transfection—MDCK-T23 cells, which stably express the tetracycline transactivator (12), were cultured in Dulbecco's modified Eagle's medium (Invitrogen) supplemented with 10% fetal bovine serum. The generation and propagation of replication-defective recombinant adenovirus encoding tetracycline-repressible influenza hemagglutinin Japan serotype (HA) is described in Ref. 13. Similar methods were used to construct adenovirus encoding tetracycline-repressible YFP-p75 (YFP appended to the cytoplasmic tail) and wild type VSV-G (Indiana strain). MDCK cells were infected with adenovirus at a multiplicity of infection of 50–100 for each virus as described previously (13), and the experiments were performed the following day.

Reconstitution of Transport Carrier Release from Perforated Cells—Protein export was reconstituted essentially as described by Ellis *et al.* (14). Briefly, cells on 10-cm dishes were incubated for 30 min at 37 °C in bicarbonate-free, cysteine-free, methionine-free Dulbecco's modified Eagle's medium and then metabolically radiolabeled for 20 min in the same medium supplemented with 50 μCi/ml Easy Tag Express Protein Labeling Mix [^{35}S] (PerkinElmer Life Sciences). The medium was then replaced with cold bicarbonate-free minimal essential medium, and the cells were incubated at 19 °C for 2 h to accumulate mature newly synthesized proteins in the TGN (15, 16). The cells were then incubated for 10 min on ice in 10 mM HEPES, pH 7.2, 15 mM KCl, and scraped into break buffer (50 mM HEPES, pH 7.2, 90 mM KCl). The buffer was adjusted to 500 mM KCl by addition of an equal volume of 50 mM HEPES, pH 7.2, 1 M KCl, and the cells were centrifuged at 800 × *g* in a Beckman GS-6R centrifuge. After washing the cell pellet with break buffer, the cells were resuspended in GGA buffer (25 mM HEPES, pH 7.4, 38 mM potassium glutamate, 38 mM potassium aspartate, 38 mM potassium gluconate, 2.5 mM $MgCl_2$, 2 mM EGTA-free acid, 1 mM dithiothreitol). Aliquots of the perforated cell suspension (25 μl) were distributed into Eppendorf tubes containing an equal volume of GGA and where indicated an ATP regenerating system and rat brain cytosol (2 mg/ml final concentration). The samples were incubated at 37 °C for 90 min and then centrifuged in a tabletop microcentrifuge at 12,000 rpm for 2 min to pellet the cells. The supernatant (containing released vesicles) and pellet (cells) were collected separately and solubilized with detergent solution (50 mM Tris-HCl, 2% Nonidet P-40, 0.4% deoxycholate, 62.5 mM EDTA, 1 μg/ml aprotinin, pH 8.0). The proteins were immunoprecipitated, and the percentage of release quantitated using a PhosphorImager. The data were analyzed using SigmaStat software (Systat), and $p < 0.05$ was considered to be statistically significant.

Protease Protection Assay—Supernatants from perforated cells reconstituted with an ATP-regenerating system and cytosol were incubated with 25 μg/ml trypsin (bovine pancreas treated with L-1-tosylamido-2-phenylethyl chloromethyl ketone; Sigma) in GGA buffer on ice, in the presence or absence of 0.05% Triton X-100. After 10 min, soybean trypsin inhibitor was added to a final concentration of 200 μg/ml. After addition of detergent solution, HA or YFP-p75 was immunoprecipitated, and the samples were analyzed after SDS-PAGE.

Immunoisolation—Supernatants from release assays were incubated with 2 μg of polyclonal anti-GFP antibody (Invitrogen-Molecular Probes) or rabbit anti-mouse IgG (Jackson ImmunoResearch) and 2×10^7 Dynabeads (M-280 sheep anti-rabbit IgG; Dynal Biotech) on a shaker for 24 h at 4 °C. The samples were washed three times with phosphate-buffered saline, 0.1% bovine serum albumin, eluted by boiling in Laemmli sample buffer, and analyzed by SDS-PAGE.

Indirect Immunofluorescence—MDCK cells were seeded onto coverslips in 12-well dishes. The following day the cells were infected with adenoviruses encoding HA or YFP-p75. After 5 h at 37 °C, the cells were incubated at 19 °C for 2 h followed by an additional hour in the presence of 100 μg/ml cycloheximide, then fixed with 4% paraformaldehyde, and permeabilized for 5 min with 0.5% Tx-100. After blocking nonspecific sites with 0.25% bovine serum albumin, the samples were incubated with primary antibodies (monoclonal anti-HA antibody Fc125 or monoclonal anti-GFP antibody (Covance) and polyclonal anti-furin antibody (Affinity BioReagents)), washed, and incubated with 2° antibodies (AlexaFluor goat anti-mouse 488 and AlexaFluor goat anti-rabbit 647). Coverslips were mounted on glass slides using ProLong Gold antifade reagent (Invitrogen-Molecular Probes) and examined using a spinning disc confocal microscope (PerkinElmer UltraVIEW). The images were acquired using Metamorph software and processed using Adobe Photoshop.

Sucrose Gradient Centrifugation—Analysis of released transport carriers by sucrose gradient sedimentation was performed using a modification of the method described in Ref. 17. A

10-ml continuous 0.4–0.6 M sucrose gradient was formed over a 1-ml cushion of 2 M sucrose in an ultraclear 12-ml centrifuge tube. Sucrose solutions were prepared in ice-cold 20 mM HEPES-KOH, pH 7.3. Released transport carriers from MDCK cells co-expressing YFPp75 and HA were diluted in 200 μl of 0.2 M sucrose and layered on top of the gradient. An additional 400 μl of 20 mM HEPES-KOH, pH 7.3, was loaded on the top of the sample, and the tubes were centrifuged at 125,000 × *g* (27,000 rpm) at 4 °C for 1 h in a TH641 rotor (Sorvall). Six 0.6-ml fractions were collected from the top followed by eight 1.0-ml fractions. The fractions were solubilized by the addition of 5-fold concentrated detergent solution, divided into two equal aliquots, immunoprecipitated using either anti-GFP antibody or anti-HA antibody, and analyzed by SDS-PAGE.

Surface Delivery of HA and YFP-p75—MDCK cells seeded onto 6-well dishes were infected with adenoviruses encoding HA or YFP-p75. The cells were then radiolabeled for 5 h with 85 μCi/ml Easy Tag Express protein labeling mix [^{35}S] in cysteine-free, methionine-free supplemented with 10% complete medium. The medium was then replaced with cold bicarbonate-free minimal essential medium, and the cells were incubated at 19 °C for 2 h followed by an additional 1 h in the presence of 100 μg/ml cycloheximide. The total amount of HA at the cell surface was determined using cell surface trypsinization as described previously (18). Surface biotinylation of YFP-p75 was performed using the method described in Ref. 19. HA was immunoprecipitated with mAb Fc125, whereas YFP-p75 was immunoprecipitated with polyclonal anti-GFP antibody. The samples were analyzed using SDS-PAGE, and surface delivery was quantitated using a PhosphorImager.

RESULTS

Data from our lab and other labs increasingly suggest that surface delivery of newly synthesized raft-associated and raft-independent markers is independently regulated and proceeds via distinct pathways. To begin to dissect these pathways, we reconstituted release of post-Golgi transport carriers containing the raft-independent apical protein YFP-p75, the raft-associated apical protein influenza HA, and the basolateral marker YFP-VSV-G. As a first step, we established conditions to accumulate mature cargo proteins intracellularly in MDCK cells. Cells cultured on plastic dishes were infected with adenoviruses encoding these proteins, radiolabeled for 20 min, and then incubated for 2 h at 19 °C. The cells were then solubilized, and cargo proteins were recovered by immunoprecipitation and treated with endoglycosidase H to assess their glycosylation status (Fig. 1*A*). Under our staging conditions, we found that radiolabeled HA and VSV-G migrated as two bands, with the upper band being resistant to digestion by endoglycosidase H. YFP-p75 also migrated predominantly as two bands; however, in some experiments a faint intermediate band was also visible. The upper band was resistant to endoglycosidase H digestion and could also be labeled with [^{35}S]sulfate, which is incorporated into mature glycans in the TGN (20, 21). In addition, we measured the cell surface expression of each radiolabeled marker. Only 5–9% of each protein was detected at the plasma membrane under our staging conditions, confirming that the 19 °C incubation effectively blocked cell surface delivery of all three proteins (not shown).

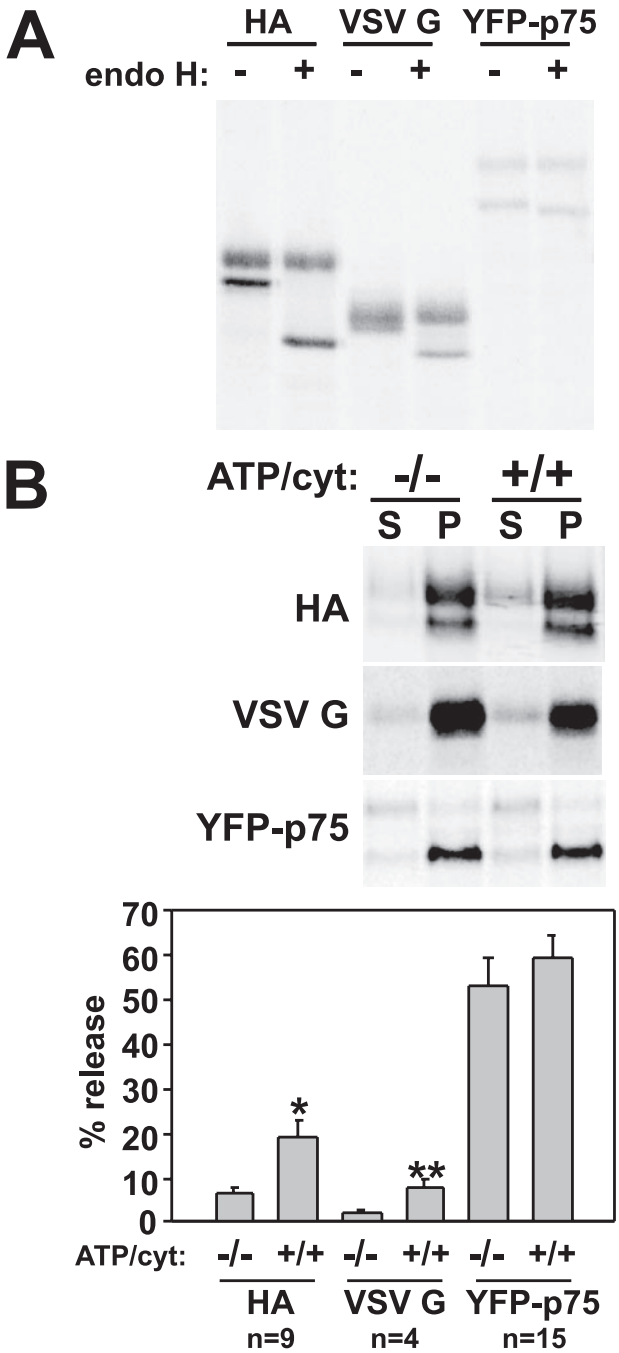

FIGURE 1. **Export characteristics of YFP-p75 are distinct from HA and VSV-G.** *A*, MDCK cells expressing HA, VSV-G, or YFP-p75 were radiolabeled for 20 min and chased for 2.5 h at 19 °C. The cells were solubilized, the cargo proteins were immunoprecipitated and treated with or without endoglycosidase H (*endo H*), and the samples were analyzed by SDS-PAGE. *B*, MDCK cells were radiolabeled and chased as above, then perforated, and incubated in the absence (−/−) or presence (+/+) of an ATP-regenerating system (*ATP*) and rat brain cytosol (*cyt*). Released transport carriers (*S*) were segregated from the cells (*P*) by centrifugation, and both fractions were solubilized and immunoprecipitated. The percentage of release of mature protein was quantitated as described under "Materials and Methods. " A typical experiment is shown for each cargo, and data from 4–15 experiments (means ± S.E.) are plotted below. *, $p = 0.008$; **, $p = 0.029$ by rank sum analysis.

To reconstitute cargo export, we radiolabeled and staged MDCK cells as above and then perforated them by scraping

after a brief incubation in hypotonic buffer. Aliquots of the perforated cell suspension were then incubated for 90 min at 37 °C in high potassium buffer in the presence or absence of an ATP-regenerating system and exogenous cytosol. Under these conditions, transport carriers are released and can be easily segregated from the cells by differential centrifugation. Using this approach, we previously demonstrated that efficient release of the mature form of HA from HeLa cells required both ATP and cytosol but was independent of coat-recruiting GTPase ADP ribosylation factors (14). Neither the nonsialylated fraction of HA nor a *trans*-Golgi resident protein were released in significant amounts under these reconstitution conditions (14).

Similar to our results in HeLa cells, upon perforation of the MDCK cells and reconstitution of transport carrier release, we routinely observed moderately efficient release of mature HA and VSV-G that was highly dependent on inclusion of ATP and cytosol during the assay (Fig. 1*B*, *upper* and *middle panels*). In contrast, release of mature YFP-p75 was largely independent of these variables (Fig. 1*B*, *lower panel*). As expected, the immature fraction of all three cargo proteins was poorly released under these reconstitution conditions. Release of mature YFP-p75 was considerably more efficient than that of HA or VSV-G. Whereas HA and VSV-G export varied between 3 and 20% of the total mature protein, we routinely observed release of between 30 and 70% of mature YFP-p75. The mean ± S.E. release of each cargo protein over 4–15 experiments is plotted in Fig. 1*B*. Similar results were obtained when the release reaction was limited to 30 min (not shown). Release of both VSV-G and YFP-p75 was reduced when the reconstitution reaction was carried out at 4 °C instead of 37 °C, and co-expression of YFP-p75 with VSV-G did not affect either the ATP/cytosol dependence or the efficiency of release of either marker (Fig. 2). Moreover, the ATP/cytosol independent release of p75 was not due to the presence of the YFP tag, as we observed similar release of untagged p75 (not shown). Inclusion of a 0.5 M salt washing step to deplete peripherally associated membrane proteins prior to reconstitution of YFP-p75 export also did not appear to affect release efficiency.[5]

We next examined whether released HA segregated with co-expressed YFP-p75 and whether the cosegregation efficiency was dependent on inclusion of ATP and cytosol in the reconstitution reaction. Export of transport carriers from MDCK cells co-expressing radiolabeled and staged HA and YFP-p75 was carried out in the absence or presence of ATP and cytosol as usual. The released cargo was separated from cells by centrifugation, and a duplicate fraction was subjected to immunoisolation using Dynabeads coupled to polyclonal anti-GFP or as a control, rabbit IgG antibodies. As shown in Fig. 3, release of mature YFP-p75 was very efficient in both the absence and presence of ATP and cytosol (79 and 84%, respectively, Fig. 3, *lanes 6–9*), whereas release of HA was ATP- and cytosol-dependent as usual (3.2% *versus* 18.1% in the absence and presence of ATP/cytosol, respectively; Fig. 3, *lanes 2–5*). YFP-p75 released under either condition was efficiently recovered using anti-GFP coupled Dynabeads (compare *lanes 12* and *13* with *lanes 6* and *8*, respectively) but not using Dynabeads coupled to nonspecific IgGs (Fig. 3, *lanes 10* and *11*). More HA was co-isolated with YFP-p75 when the reconstitution included ATP and cytosol (HA band in *lanes 12* and *13*), but in each case this represented a similar fraction (~20%) of the total released HA.

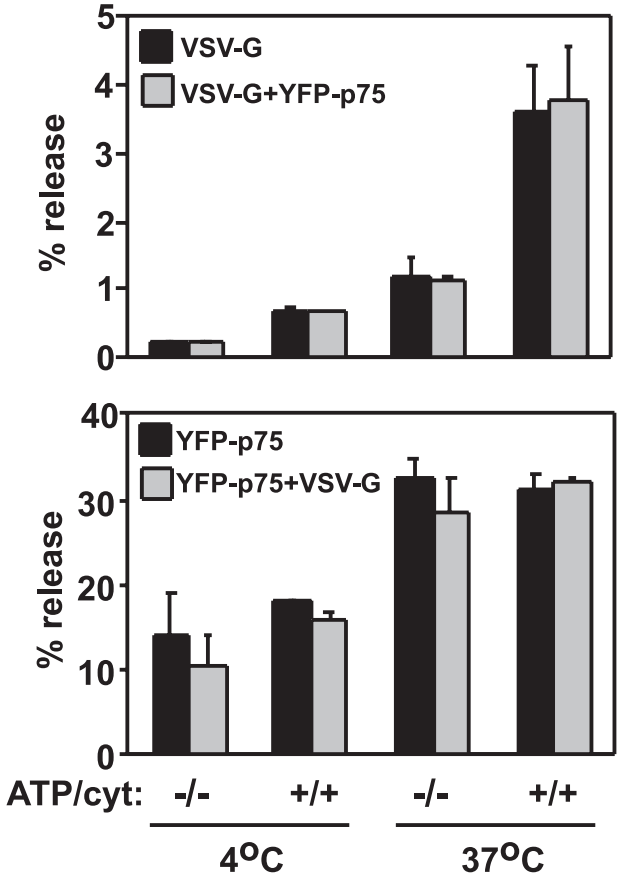

FIGURE 2. **VSV-G release is unaffected by co-expression of YFP-p75.** VSV-G and YFP-p75 were co-expressed in MDCK cells, radiolabeled, and chased as above, and transport carrier export from permeabilized cells was reconstituted at 4 and 37 °C in the presence or absence of ATP and cytosol. Duplicate samples were immunoprecipitated using anti-VSV-G or anti-GFP antibodies.

Analysis of YFP-p75-containing Transport Containers—We next compared the sedimentation and latency characteristics of HA and YFP-p75 released from MDCK cells. Formation of transport carriers was reconstituted in the presence of ATP and cytosol from cells co-expressing both cargo proteins, and the supernatant fraction was loaded on top of linear 0.4–0.6 M sucrose gradients. After centrifugation for 1 h at 125,000 × *g*, the aliquots were collected and immunoprecipitated to recover YFP-p75 and HA. As shown in Fig. 4*A*, the two markers had very different sedimentation profiles. HA was recovered in a broad peak centered on fraction 5 of the gradient. In contrast, the majority of mature YFP-p75 was recovered in the top fractions with some diffusion into later fractions, whereas immature YFP-p75 was recovered largely in the pellet.

To determine whether YFP-p75 and HA were released in intact membrane carriers, we evaluated the accessibility of the lumenal domains of released cargoes to exogenously added trypsin. Supernatants from a reconstitution reaction performed in the presence of ATP and cytosol were incubated with trypsin

[5] Y. Lai, unpublished results.

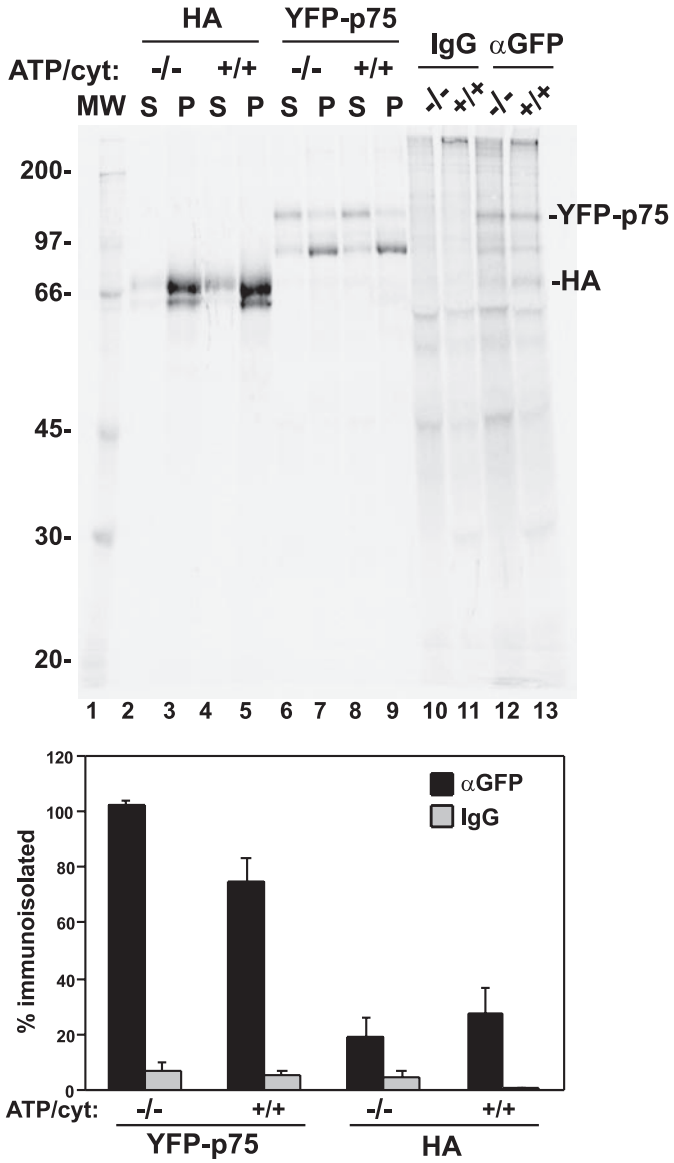

FIGURE 3. **YFP-p75 and HA do not co-immunoisolate.** MDCK cells co-expressing HA and YFP-p75 were radiolabeled for 20 min and incubated at 19 °C for 2.5 h. The cells were perforated, and export of transport carriers was reconstituted in the absence (−/−) or presence (+/+) of ATP and cytosol (*cyt*, *lanes 2–9*). Released carriers (*S lanes*) were separated from cells (*P*) by centrifugation. The percentage of release in this experiment was HA (−/−): 3.2%; HA (+/+): 18.1%; YFP-p75 (−/−): 79%; YFP-p75 (+/+): 84%. Duplicate S fractions (equivalent to *lanes 2*, *4*, *6*, and *8*) were incubated with Dynabeads coupled to polyclonal anti-GFP or rabbit IgG to recover YFP-p75-containing membranes, then washed, and eluted in Laemmli sample buffer (*lanes 10–13*). The samples were analyzed by SDS-PAGE; molecular mass standards (*MW*) were loaded in the *left-most lane*. YFP-p75 immunoisolation efficiency and HA co-isolation efficiency were quantitated as the percentage of recovered relative to the matched S sample in *lanes 2–9*. The gel shows a single experiment; the graph below shows the averages ± range of two independent experiments. The migration of molecular mass standards (in kDa) is shown in *lane 1*. More HA was co-isolated with YFP-p75 when the reconstitution included ATP and cytosol, but in each case this represented a similar fraction (~20%) of the total released HA.

in the presence or absence of Triton X-100 for 10 min. After the addition of soybean trypsin inhibitor, detergent-containing solution was added, and the samples were immunoprecipitated using antibodies recognizing lumenal epitopes of HA or p75 and then analyzed by SDS-PAGE (Fig. 4*B*). As we previously observed in HeLa cells, released HA was largely insensitive to trypsin treatment in the absence of Triton X-100; however, in the presence of detergent, the characteristic trypsin cleavage of HA into two fragments was observed. In contrast, YFP-p75 was quantitatively cleaved into lower molecular weight forms even in the absence of detergent.

HA and p75 Accumulate in Distinct Intracellular Compartments at Low Temperature—The dramatic differences in release characteristics of mature HA and YFP-p75 led us to wonder whether they might be segregated into distinct subdomains of the Golgi complex prior to reconstitution. Because indirect immunofluorescence reveals the localization of the entire cellular cohort of a given protein, whereas our *in vitro* experiments monitor the trafficking of only a radiolabeled subset of protein, we first established expression conditions that would minimize surface expression of each cargo while maximizing the accumulation of mature protein intracellularly. Using these circumstances, we should be able to determine the intracellular distribution of cargo staged under conditions similar to those used in our *in vitro* assays above. To this end, we expressed HA, YFP-p75, or VSV-G proteins in MDCK cells for short periods (5 h) and then incubated the cells for 3h at 19 °C. Cycloheximide was included during the last hour at 19 °C to inhibit synthesis of additional protein. The cells were then fixed and processed for indirect immunofluorescence to examine the localization of each cargo relative to the TGN marker furin and to each other (Fig. 5). The intracellular cohort of YFP-p75 localized in structures that were closely associated but not always coincident with furin-positive compartments, consistent with efficient staging in the Golgi/TGN (Fig. 5*A*, *row a*). VSV-G expressed under these conditions also co-localized partly with furin (Fig. 5*A*, *row b*). In contrast, intracellular HA was found largely in more dispersed structures, some of which were closely apposed to but clearly distinct from furin-positive compartments (Fig. 5*A*, *row c*). Co-localization of co-expressed YFP-p75 and HA confirmed that the two markers accumulate in distinct compartments after incubation at 19 °C (Fig. 5*A*, *row d*).

To determine the fraction of each cargo that was mature and present at the cell surface under these expression conditions, we expressed HA, or YFP-p75 in MDCK cells as above and included [^{35}S]Met during the entire expression period to radiolabel the total cohort of protein expressed. Subsequent to the 19 °C staging period, the cells were either biotinylated (p75) or trypsinized (HA) and then solubilized. Each cargo protein was recovered by immunoprecipitation, and the mature and cell surface fractions were determined after SDS-PAGE (Fig. 5*B*). Under these conditions, ~82% of the total HA was mature, whereas only 13% had reached the cell surface, similar to the radiolabeled protein we followed in our *in vitro* assays (5% of total). Thus, the intracellular distribution we observed under these expression conditions is representative of the mature radiolabeled protein whose export we monitored in our *in vitro* assays. Similarly the distribution of YFP-p75 under these expression conditions (74% mature, 8% at the cell surface) was comparable with the cohort radiolabeled in our *in vitro* experiments.

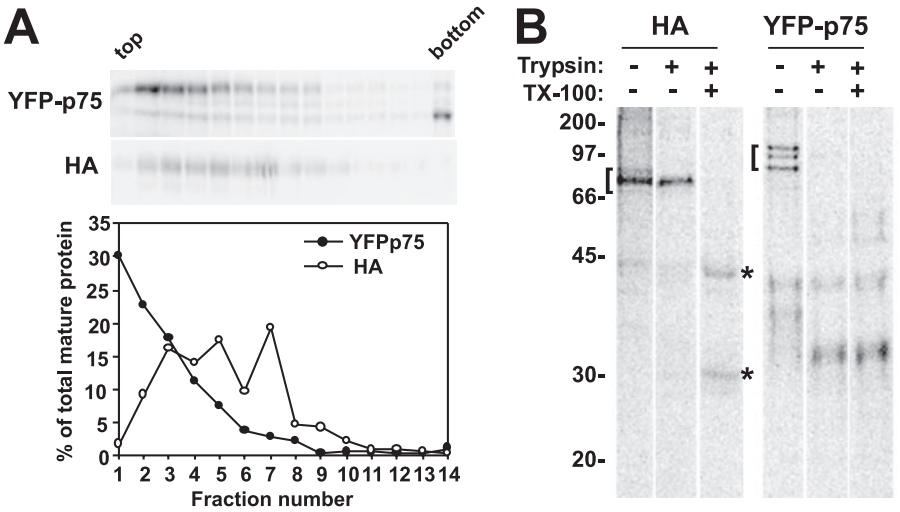

FIGURE 4. **Characterization of p75-containing transport containers.** MDCK cells co-expressing YFP-p75 and HA were radiolabeled for 20 min, chased for 2.5 h at 19 °C, then perforated and incubated in the presence of ATP and cytosol. Released transport carriers were loaded onto 0.4–0.6 M linear sucrose gradients and centrifuged at 125,000 × *g* for 1 h. Six 0.6-ml fractions were collected from the top, and then eight 1.0-ml fractions were collected from the top and solubilized. Each fraction was divided into two equal aliquots that were immunoprecipitated to recover YFP-p75 and HA and analyzed by SDS-PAGE. The distribution of the *mature* form of HA and YFP-p75 (percentage of total in each fraction) is plotted beneath the gel for each protein. Similar results were obtained in two independent experiments. *B*, released transport carriers from perforated cells expressing HA or YFP-p75 were incubated with trypsin in the presence or absence of TX-100 and immunoprecipitated using anti-HA or anti-p75 antibodies (both antibodies recognize luminal epitopes). The samples were analyzed by SDS-PAGE. Bands representing full-length HA and YFP-p75 forms are indicated by *brackets*, and the migration of molecular mass markers (in kDa) is shown on the *left*. HA is largely trypsin resistant in the absence of detergent and is cleaved into HA1 and HA2 fragments (marked by *asterisks*) in the presence of TX-100. In contrast, YFP-p75 is quantitatively degraded even in the absence of detergent.

DISCUSSION

In this study we have reconstituted *in vitro* the export of two intracellularly staged apical markers and a basolateral marker expressed in renal epithelial cells. We found that that the requirements for release of the raft-associated protein influenza HA are dramatically different from those of the raft-independent marker YFP-p75. In addition, the two markers are released in distinct transport carriers with different morphology. These transport carriers appear to originate from distinct membrane domains, because YFP-p75 and HA accumulate in distinct intracellular compartments when "staged" at 19 °C. Together our data suggest that the intrinsic properties of these proteins modulate their distribution into distinct microdomains with very different characteristics. Our data are consistent with biochemical and live cell imaging studies that demonstrate differential trafficking of these markers in intact cells and suggest that this assay may provide a useful approach to identify specific components involved in the formation of each type of carrier.

A striking observation in our *in vitro* reconstitution assay was that release of intracellularly staged YFP-p75 was extremely efficient and was essentially independent of ATP and cytosol. Importantly, only the mature (sialylated) form of YFP-p75 was released under these conditions. In contrast, release of two other cargo proteins, HA and VSV-G, was highly dependent on addition of an ATP-regenerating system and cytosol. Expression of YFP-p75 did not affect release characteristics of co-expressed HA or VSV-G.

We previously showed that HA is released from HeLa cells in intact transport carriers with an average diameter of 86 nm (14). In contrast, our current studies demonstrate that released YFP-p75 is recovered in membrane fragments rather than intact transport carriers, because the lumenal domain of the protein was susceptible to proteolytic digestion. Moreover, released YFP-p75 did not sediment in sucrose gradients, in contrast to released HA. Based on these observations, we hypothesize that YFP-p75 is released from the Golgi in fragile tubules that disintegrate during the segregation of cells from released carriers. Because cytosolic proteins are not required for efficient release of YFP-p75, it appears that these tubules form via a coat-independent mechanism. Indeed, the Golgi complex has previously been demonstrated to form an extensive tubular network under low ATP conditions *in vivo* or upon incubation of isolated Golgi membranes with brefeldin A (22). Importantly, the post-Golgi release of YFP-p75 in tubular compartments is consistent with results of live cell imaging studies, which demonstrated extensive partitioning of YFP-p75 into Golgi-derived tubules (23).

The differential release characteristics of HA and YFP-p75 reflects their accumulation at distinct intracellular sites upon staging at 19 °C. Under expression conditions where the total cohort of protein mimics the distribution of radiolabeled protein followed in our reconstitution assay, we observed that "staged" YFP-p75 co-localized largely with or near the TGN marker furin. In contrast, HA was localized to distinct structures that were not coincident with YFP-p75 or furin staining. These compartments may represent subdomains of the TGN, or less likely, a distinct but closely associated post-Golgi compartment. Live cell and biochemical experiments have previously suggested some segregation of staged apical and basolateral proteins within the Golgi complex (24, 25). To our knowledge, this is the first example where two apical proteins have been found to segregate within this compartment.

There is precedence for the existence of distinct subcompartments of the TGN based on differential localization of coat proteins (26–28). However, our previous and current studies suggest that both HA and YFP-p75 may be exported from the TGN in uncoated transport carriers (14). Thus, there may be additional microdomains within the TGN that form independently of coat association. *In vitro* studies have demonstrated that tubules emanating from liposomes or purified Golgi membranes have a composition distinct from that of the remaining vesicular regions (29). Segregation or localized synthesis of lipids generates domains distinct from the classic glycolipid-enriched lipid rafts could thus facilitate the accumulation of spe-

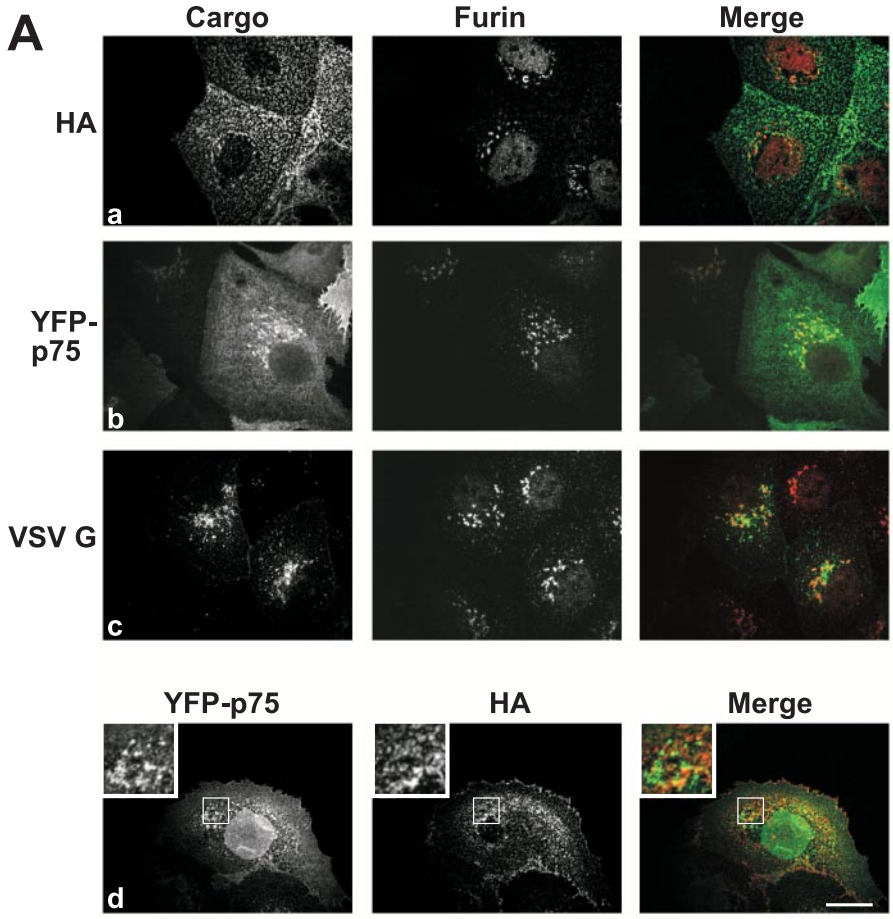

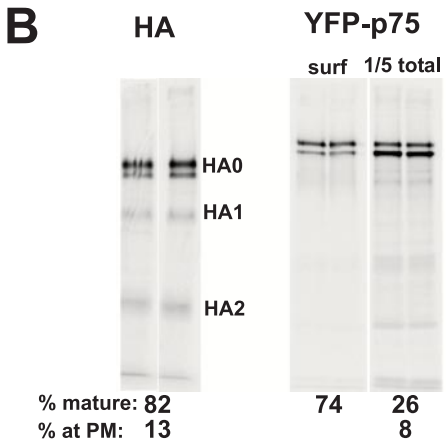

FIGURE 5. **YFP-p75 and HA do not co-localize intracellularly after low temperature staging.** MDCK cells were infected with adenoviruses encoding YFP-p75, VSV-G, and/or HA for 1 h and then incubated for 5 h at 37 °C and 3 h at 19 °C. Cycloheximide was included during the last hour at 19 °C. The cells were then fixed and processed for immunofluorescence to detect each marker and furin (*rows a–c*) or to visualize co-expressed HA and YFP-p75 (*row d*). The *insets* in *row d* show enlarged versions of the *boxed regions*. Individual confocal sections and a merged image are shown for each condition. *Scale bar*, 30 μM. The nuclear fluorescence in the YFP-p75 panel in *row d* represents background from the polyclonal anti-GFP used in this sample. In contrast, cells in *row b* were labeled using a monoclonal anti-GFP antibody; in both cases, this protocol was used to amplify the fluorescent signal for p75 over that provided by the YFP moiety (see "Materials and Methods"). *B*, MDCK cells were radiolabeled starting immediately after adenoviral infection and incubated as described in *A*. At the end of the 19 °C incubation, the cells were biotinylated or treated with trypsin to mark cell surface YFP-p75 or HA, respectively, and then solubilized and cargo proteins immunoprecipitated. One-fifth of the total YFP-p75 was reserved to calculate *total* and biotinylated YFP-p75 was recovered from the remainder using streptavidin-agarose (*surf lanes*). The migration of full-length HA (*HA0*) and HA trypsin fragments (*HA1* and *HA2*) is noted. The maturation and cell surface delivery of each cargo was quantitated after SDS-PAGE as described under "Materials and Methods. " A small fraction of the YFP-p75 recovered at the surface is in the immature form; we have previously observed similar results in both HeLa and MDCK cells; however, this represents only 3% of the total immature YFP-p75 in the cell.

cific cargo at specific sites in the Golgi complex and in other organelles.

How does the distinct staging and export of YFP-p75 and HA relate to the trafficking routes of these cargoes? We have previously found that raft-associated and raft-independent proteins take distinct routes to the apical membrane, with raft-independent proteins traversing the rab11-positive apical recycling endosomes and raft-associated proteins apparently intersecting a distinct apical endocytic compartment (9). Our data demonstrating segregation and differential export of YFP-p75 and HA from distinct subcompartments of the TGN is consistent with the notion that multiple types of transport carriers with different destinations can bud from the TGN. Indeed, recent studies in yeast and mammalian cells have suggested roles for several novel coat proteins in the formation of transport carriers enriched in selective cargoes (28, 30–32).

What is the purpose of having so many different pathways to the cell surface? Presumably this allows for finer regulation of protein delivery and secretion in response to physiological stimuli. For example, the cells may favor production of a particular type of transport carrier in response to metabolic stress. Based on our studies, one might hypothesize that formation of tubules is preferentially favored when cellular ATP levels are low, and this might favor delivery of specific proteins required to maintain viability under these stressed conditions. Alternatively, changes in transport carrier morphology and cargo segregation in response to the prevailing metabolic conditions may explain the discrepant observations of several live cell imaging studies. Whereas some studies have suggested that cargoes are efficiently segregated into distinct transport carriers that appear to emanate directly from the TGN (24, 33), others have concluded that cargo exits the TGN in large structures that subsequently gave rise to individual carriers con-

taining sorted cargo (6, 34, 35). Clearly, future studies will be required to more clearly dissect how biosynthetic transport is regulated and whether cargo sorting and transport carrier morphology are altered in response to changes in cell metabolism and signaling.

Acknowledgments—We thank Ed Cluett for helpful discussion and Gerard Apodaca and Giovanni Ruiz for assistance with related unpublished studies.

REFERENCES

1. Rodriguez-Boulan, E., Kreitzer, G., and Müsch, A. (2005) *Nat. Rev. Mol. Cell Biol.* **6,** 233–247
2. Ellis, M. A., Potter, B. A., Cresawn, K. O., and Weisz, O. A. (2006) *Am. J. Physiol.* **291,** F707–F713
3. Potter, B. A., Hughey, R. P., and Weisz, O. A. (2006) *Am. J. Physiol.* **290,** C1–C10
4. Lin, S., Naim, H. Y., Rodriguez, A. C., and Roth, M. G. (1998) *J. Cell Biol.* **142,** 51–57
5. Helms, J. B., and Zurzolo, C. (2004) *Traffic* **5,** 247–254
6. Jacob, R., and Naim, H. (2001) *Curr. Biol.* **11,** 1444–1450
7. Jacob, R., Heine, M., Alfalah, M., and Naim, H. Y. (2003) *Curr. Biol.* **13,** 607–612
8. Guerriero, C. J., Weixel, K. M., Bruns, J. R., and Weisz, O. A. (2006) *J. Biol. Chem.* **281,** 15376–15384
9. Cresawn, K. O., Potter, B. A., Oztan, A., Guerriero, C. J., Ihrke, G., Goldenring, J. R., Apodaca, G., and Weisz, O. A. (2007) *EMBO J.* **26,** 3737–3748
10. Ang, A. L., Taguchi, T., Francis, S., Folsch, H., Murrells, L. J., Pypaert, M., Warren, G., and Mellman, I. (2004) *J. Cell Biol.* **167,** 531–543
11. Gravotta, D., Deora, A., Perret, E., Oyanadel, C., Soza, A., Schreiner, R., Gonzalez, A., and Rodriguez-Boulan, E. (2007) *Proc. Natl. Acad. Sci. U. S. A.* **104,** 1564–1569
12. Barth, A. I. M., Pollack, A. L., Altschuler, Y., Mostov, K. E., and Nelson, W. J. (1997) *J. Cell Biol.* **136,** 693–706
13. Henkel, J. R., Apodaca, G., Altschuler, Y., Hardy, S., and Weisz, O. A. (1998) *Mol. Biol. Cell* **8,** 2477–2490
14. Ellis, M. A., Miedel, M. T., Guerriero, C. J., and Weisz, O. A. (2004) *J. Biol. Chem.* **279,** 52735–52743
15. Fuller, S. D., Bravo, R., and Simons, K. (1985) *EMBO J.* **4,** 297–307
16. Matlin, K. S., and Simons, K. (1983) *Cell* **34,** 233–243
17. Simon, J.-P., Ivanov, I. E., Adesnik, M., and Sabatini, D. D. (2000) *Methods* **20,** 437–454
18. Henkel, J. R., and Weisz, O. A. (1998) *J. Biol. Chem.* **273,** 6518–6524
19. Altschuler, Y., Kinlough, C. L., Poland, P. A., Apodaca, G., Weisz, O. A., and Hughey, R. P. (1999) *Mol. Biol. Cell* **11,** 819–831
20. Karaivanova, V. K., and Spiro, R. G. (1998) *Biochem. J.* **329,** 511–518
21. Yeaman, C., Burdick, D., Muesch, A., and Rodriguez-Boulan, E. (1998) in *Cell Biology: A Laboratory Handbook* (Celis, J. E., ed) 2nd Ed., pp. 237–245, Academic Press, San Diego
22. Cluett, E. B., Wood, S. A., Banta, M., and Brown, W. J. (1993) *J. Cell Biol.* **120,** 15–24
23. Kreitzer, G., Marmorstein, A., Okamoto, P., Vallee, R., and Rodriguez-Boulan, E. (2000) *Nat. Cell Biol.* **2,** 125–127
24. Keller, P., Toomre, D., Diaz, E., White, J., and Simons, K. (2001) *Nat. Cell Biol.* **3,** 140–149
25. Alfalah, M., Wetzel, G., Fischer, I., Busche, R., Sterchi, E. E., Zimmer, K. P., Sallmann, H. P., and Naim, H. Y. (2005) *J. Biol. Chem.* **280,** 42636–42643
26. Ladinsky, M. S., Kremer, J. R., Furcinitti, P. S., McIntosh, J. R., and Howell, K. E. (1994) *J. Cell Biol.* **127,** 29–38
27. Derby, M. C., van Vliet, C., Brown, D., Luke, M. R., Lu, L., Hong, W., Stow, J. L., and Gleeson, P. A. (2004) *J. Cell Sci.* **117,** 5865–5874
28. Derby, M. C., and Gleeson, P. A. (2007) *Int. Rev. Cytol.* **261,** 47–116
29. Roux, A., Cuvelier, D., Nassoy, P., Prost, J., Bassereau, P., and Goud, B. (2005) *EMBO J.* **24,** 1537–1545
30. Wang, C. W., Hamamoto, S., Orci, L., and Schekman, R. (2006) *J. Cell Biol.* **174,** 973–983
31. Lock, J. G., Hammond, L. A., Houghton, F., Gleeson, P. A., and Stow, J. L. (2005) *Traffic* **6,** 1142–1156
32. Lieu, Z. Z., Lock, J. G., Hammond, L. A., La Gruta, N. L., Stow, J. L., and Gleeson, P. A. (2008) *Proc. Natl. Acad. Sci. U. S. A.* **105,** 3351–3356
33. Kreitzer, G., Schmoranzer, J., Low, S. H., Li, X., Gan, Y., Weimbs, T., Simon, S. M., and Rodriguez-Boulan, E. (2003) *Nat. Cell Biol.* **5,** 126–136
34. Polishchuk, E. V., Di Pentima, A., Luini, A., and Polishchuk, R. S. (2003) *Mol. Biol. Cell* **14,** 4470–4485
35. Polishchuk, R. S., San Pietro, E., Di Pentima, A., Tete, S., and Bonifacino, J. S. (2006) *Traffic* **7,** 1092–1103